

Accuracy of antepartum ultrasound in evaluating placental pathology using superb microvascular imaging: main research article

Natsumi Furuya¹, JUNICHI HASEGAWA², Masatomo Doi², Junki Koike², and Nao Suzuki³

¹Sei Marianna Ika Daigaku

²St. Marianna University School of Medicine

³Affiliation not available

December 21, 2020

Abstract

Objectives: To clarify whether microvascular ultrasound Doppler (SMI: superb microvascular imaging) can detect antenatal histological findings in pathologic placentas. **Methods:** In this prospective diagnostic observational study (STROBE), pregnant women who were admitted to our perinatal center for perinatal management were enrolled. Ultrasound examinations to identify placental pathologies using SMI were performed before delivery. After delivery, the placental tissue was clipped for microscopic examination, as the location of the placenta obtained ultrasound findings. The accuracy of antenatal ultrasound detection of placental pathologies was compared between women who were admitted due to fetal growth restriction (FGR), pre-eclampsia, and other indications. **Results:** The highest accuracy was observed with placental infarction in FGR (positive predictive value [PPV], 100%; sensitivity, 89%; area under the curve [AUC], 0.945), whereas PPV, sensitivity, and AUC in cases of preeclampsia were relatively low (AUC 0.540). Additionally, PPV, sensitivity, and AUC for avascular villi were 100%, 57%, and 0.785 in cases with FGR, 67%, 67%, and 0.780 in cases with preeclampsia, and 80%, 80%, and 0.920, respectively. The diagnostic accuracies predictive of congestion of stem villi and chorangiosis were insufficient (AUC<0.700). **Conclusions:** SMI can accurately detect placental pathologic findings, such as placental infarction and avascular villi. This modality may improve the perinatal management in cases of placental abnormalities.

Introduction

Superb microvascular Imaging (SMI), a recent blood flow imaging technique produced by Canon Medical Systems (Japan), employs a unique algorithm to minimize motion artifacts by eliminating signals based on the analysis of tissue movement. Compared to the conventional color Doppler imaging methods, SMI can significantly better visualize low-velocity blood flow in small vessels¹, which allows depiction of the pathology and diagnoses of placental abnormalities. Placental pathological examination is retrospectively performed after delivery to evaluate placental abnormalities that could have resulted in complications during pregnancy. However, if it is possible to predict the pathological findings antenatally using ultrasound examination, it would be useful to understand the disease state and predict the prognosis. Therefore, we investigated the evaluation of placental pathologic findings using SMI.

Using SMI, in a normal placenta, villous blood vessels can be visualized from the umbilical cord insertion to the stem villi and terminal villi. Additionally, slow blood flow in the intervillous space from the spiral artery is also visualized as a "scatter" that matches the heart rate of the mothers. In contrast, we previously demonstrated, in placenta increta, not only the thin myometrium with invasive placental tissue, but also the avascularity of the peripheral villous tree and congested stem vessels using SMI².

Furthermore, in a pilot study, we demonstrated various placental pathological findings antenatally using SMI and compared them with placental pathological findings³. According to our investigations, pathologically confirmed placental infarctions are expressed in echo-free space without both villous trees and background scatters. In cases of avascular villi, only background 'scatter' was expressed in SMI. Consequently, it was confirmed that the findings of SMI match the pathological findings.

In the present study, in order to demonstrate objectivity and reproducibility, the diagnostic accuracies of various ultrasound findings of the pathologic placenta were evaluated. The aim of the present study was to clarify the accuracy of antenatal ultrasound evaluation using SMI for placental pathological findings.

Methods

Patient population

In this prospective, diagnostic observational study, pregnant women who were admitted to our perinatal center for perinatal management between March 2019 and February 2020 were enrolled. Placental ultrasound evaluation using SMI was performed during pregnancy every 1–2 weeks. Therefore, the SMI findings in the present analysis were of those within 1–2 weeks before delivery. The findings on SMI were compared to those of the placenta submitted for pathological examination.

Ultrasound findings using SMI

Ultrasound examinations in the present study were performed by two authors (NF and JH). The placenta and umbilical cord were evaluated using B-mode to detect gross abnormalities, such as velamentous cord insertion, hyper-coiled cord, and entanglement. The placenta was then evaluated precisely using SMI from the decidual layer to the chorionic plate. When some ultrasound findings were found, the exhibited findings were mapped to the respective location on the placenta based on the location and form of the placenta and the spatial relationship with the umbilical cord insertion site.

In the normal findings of the placenta using SMI, the villous trees are identified on the fetal side—from the umbilical cord insertion to the stem villi—connecting to the terminal villi into the maternal side. Tertiary stem vessels in the villous tree are homogenous and sharply diminished. Additionally, maternal blood flow from the spiral artery is observed as 'scatter' in the intervillous space (**Figure 1, Appendix S1**). In contrast, abnormal findings were defined as follows.

Infarction

Since both the villous blood vessels and intervillous space disappear, both the background "scatter" and "villous tree" are not detected, thus, resulting in an echoic space (**Figure 2a, Appendix S2**).

b. Avascular terminal villi

Since only the villous blood flow is absent but the intervillous space is present, only the background "scatter" is observed without normal villous trees (**Figure 2b, Appendix S3**).

c. Dilatation of stem villi (Congestion)

Congestion of the stem vessels as an SMI finding is defined as clearly dilated stem villi compared with the surrounding villous stem vessels

(**Figure 2c, Appendix S4**).

Hyper-vascular terminal villi (Chorangiosis)

Chorangiosis as a SMI findings is defined as high-echoic terminal villi compared with the standard villi and appear "fluffy". (**Figure 2-d, Appendix S5**).

The ultrasound equipment used in the present study was an Aplio i700 with 1–8 MHz Convex probe (Canon Medical Systems, Japan). Setting for visualization in B-mode and SMI, including gain, dynamic range,

PRF (Pulse Repectition Frequency), and Doppler sensitivity were preliminarily adjusted and determined for placental evaluation. The investigation in each case was performed using these preset parameters.

Pathological findings

After delivery, the placental tissue was clipped for microscopic examination in the locations according to ultrasonically mapped and macroscopic investigation of the placenta. The following pathological findings were histologically confirmed in the placenta after delivery. Pathological examinations were performed by obstetricians and pathologists (NF, JH, MD, and KJ).

a. Infarction

Infarctions reveal a collapse of the intervillous space with associated villous aggregation and coagulative necrosis, and all nuclear structures disappear over time. They are accompanied by neutrophil infiltration

(**Figure 3a**).

b. Avascular terminal villi

Villous stromal-vascular karyorrhesis villi with disappearance of all blood vessels and **uniformly fibrotic and vitrified** stroma

(**Figure 3b**).

d. Dilatation of stem villi

Dilatation of stem villi is defined as an enlargement of a stem villous vessel to > 4 times that of neighboring vessels of similar caliber (**Figure 3c**).

c. Hyper-vascular terminal villi

At least 10 or more blood vessels are found in one terminal or intermediate villus; 10 or more of these villi are found in a visual field at 10x and 10 or more of them are found in [?] 3 random cotyledon sections (**Figure 3d**).

Accuracy analysis

Diagnostic sensitivity and specificity as well as positive (PPV) and negative (NPV) predictive values of ultrasound findings and pathological findings were calculated. Receiver operating characteristics (ROC) curves were generated to estimate the diagnostic accuracy of each finding using the area under the binomial ROC curve (AUC).

Analysis of intra- and inter-observer error

SMI findings in pathological placentas were used to calculate the inter-observer agreement. An inter-observer error was determined by examining the four types of findings between the two examiners (NF and JH) in 22 findings. Additionally, an inspector (NF) evaluated the findings of 22 places as 4 types of findings twice at intervals, and calculated the intra-observer error.

Ethics statement

This study was approved by the ethics board of St. Marianna University School of Medicine, Kawasaki, Japan (No. 4543; Sep. 27, 2019). This investigation was conducted in accordance with the principles of the Declaration of Helsinki. Written informed consent was obtained from all patients.

Results

The pre-evaluated κ -values of inter- and intra-observer errors were 0.76 and 0.88, respectively. Thirty-four pregnant women admitted to the MFICU (Maternal-fetal intensive care unit) in our hospital were enrolled. The characteristics of the participants are presented in **Table 1**. The median maternal age was 33.5 years. The participants included 19 cases of FGR and/or preeclampsia and 15 cases of admissions due to other

indications; in these cases, the median gestational age at ultrasound examination was 34 and 33 weeks of gestation, respectively.

The comparisons of SMI findings with histological findings are presented in **Table 2**. The accuracy of antenatal ultrasound detection of placental pathological findings and ROC curves are presented in **Table 3 and Figure 4**. The most accurate diagnostic finding was placental infarction in cases with FGR (PPV, 100%; sensitivity, 88.9%; AUC, 0.945), whereas PPV, sensitivity, and AUC in cases with preeclampsia were relatively low. PPV, sensitivity, and AUC for avascular villi were 100%, 57.1%, and 0.785 in cases with FGR, 66.7%, 66.7%, and 0.780 in cases with preeclampsia, and 80%, 80%, and 0.920, respectively.

Discussion

Main findings

Main outcomes in the present study is placental pathological findings, especially, infarction and avascular villi, could be detected during pregnancy with high PPV using SMI.

Strength and limitation

The limitations of the current study are that the results were examined based on subjective evaluation of both SMI and pathology, although pathologic evaluations are usually performed based on subjective evaluations. While it is considered that a certain degree of consensus is achieved between pathologists regarding the pathological findings, there is no established consensus for diagnosing using SMI even though few inter-observer errors have been established. Previous studies have quantitatively evaluated placental Doppler intensity, such as vascular index and flow index⁴. Conventional color Doppler detects both villous blood flow and gross intervillous blood flow. However, we believe that the strength of placental pathological evaluation using SMI is that the blood flow from the mother and fetus can be distinguished. The method of qualitative evaluation based on the pathology, instead of quantitative evaluation, would be more exact and useful in the perinatal management of placental abnormalities.

Interpretation

Early onset preeclampsia and placenta-related FGR are associated with incomplete transformation of the spiral arteries, which result in hypoperfusion of the placenta and induced placental infarction^{5, 6}. SMI is good for visualizing minute blood flow; therefore, it can easily help identify lesions of placental infarction as lack of vascularity surrounding normal placental blood flow. In contrast, in tissues with avascular villi, only capillaries are absent in the villous tissue⁷, which is not distinguishable from normal placenta using B-mode ultrasound. Even with conventional color Doppler, it is difficult to visualize the minute blood flow of the capillaries in the terminal villi. If the flow velocity range is lowered to detect such minute flow, motion artifacts would disturb the expression of real blood flow. However, SMI enables the expression of such thin and sharp terminal villous blood vessels. Therefore, ultrasound diagnosis of avascular villi can be established by identifying the presence of slow congested maternal blood flow in the intervillous space with absent peripheral villous blood vessels. We believe that this is a breakthrough outcome of the current study.

Maternal vascular malperfusion, such as pre-eclampsia and FGR, cause utero-placental hypoxic disorder due to incomplete remodeling of the spiral arteries in the first trimester, thus, resulting in placental infarction⁸. Isolated small infarcts can be found pathologically in uncomplicated pregnancies; however, multiple central infarcts often associated with intervillous fibrin deposition are found in severe preeclampsia and FGR⁷. Although conventional ultrasound can detect these large lesions as complex echogenic intra-placental masses close to the basal plate⁹, SMI enables the detection of these small lesions even in tertiary villous tissues. However, the diagnostic accuracy for predicting infarction and avascular villi using SMI was higher in cases with FGR than that in cases with pre-eclampsia. Cases more adversely affected by maternal malperfusion, such as those with FGR and preeclampsia, are likely to have many and/or large pathologic findings in the placenta, which we believe might be the reason that much larger lesions could be easily detected. Diffuse small infarctions might be difficult to distinguish from avascular villi expressed as scatter without villous trees (**Figure 5, Appendix S6**).

Contrary to maternal vascular malperfusion, occlusion or compression of the umbilical cord, such as hypercoiled cord, can cause a dilation of stem villi⁷. Consequently, fetal vascular malperfusion, which is characterized by thrombosis and ischemic villi due to umbilical cord blood flow stasis result in FGR¹⁰. Therefore, in cases of FGR, we hypothesized that various placental causes of FGR, both maternal and fetal vascular malperfusion, could be distinguished using SMI. We focused on the dilatation of stem villi as one of the findings of fetal vascular malperfusion; however, the accuracy of ultrasound diagnosis was low. Since SMI is an ultrasound Doppler method, SMI blood flow image can be easily enhanced. Furthermore, in histological evaluation, the slice of the tissue does not always include the cross section of the blood vessel in the center. Therefore, we believe the discrepancy between the ultrasound findings and sliced histological findings to be large. The findings of congestion in stem villi are relatively large compared to the other findings in the present study. In such a large vascular evaluation, comparison between the B-mode ultrasound and macroscopic placental findings might be superior to the comparison between SMI and histological findings.

Placental histological findings of chorangiosis are often investigated in the placenta in cases of preeclampsia. Chorangiosis is believed to form due to an adaptive response to placental hypoxia¹¹. In the present study, we defined chorangiosis as an ultrasonographic finding when the Doppler strength of SMI was higher than that of the surrounding villi. However, it was difficult to distinguish the exact chorangiosis from normal placental tissue. We believe that this is because of the relative comparison of echogenicity with the standard villous findings. Originally, the diagnosis of chorangiosis should be pathologically made when hyperbranching is confirmed¹². Radically, we noticed that the definition of ultrasound findings of chorangiosis should be reconsidered.

Conclusion

The diagnostic accuracy of antenatal ultrasound diagnosis in predicting the placental pathology using SMI is guaranteed in placental infarction and avascular villi. We believe that prospective determination of maternal or fetal vascular malperfusion or problems with terminal villi formation during pregnancy using the present method can improve the perinatal management in the future.

Acknowledgments

Author contributions : NF and JH conceived the study. NF and JH drafted the initial protocol, analyzed the data, and prepared the first draft of the manuscript. All authors collected data and analyzed each maternal death. NF and JH coordinated the study and developed the database and analyzed the data. All authors contributed to the drafting of the manuscript. JH, MD, JK and NS are the guarantors for the study. All authors had full access to all of the data in the study and take responsibility for the integrity of the data and the accuracy of the data analysis.

Competing financial Interest statement: All authors declare that they have no conflict of interest.

Data availability: The data related to this study was collected from medical records, paying attention to confidentiality.

Ethical approval and informed consent: All procedures performed in studies involving human participants were in accordance with the ethical standards of the institutional and/or national research committee and with the 1964 Helsinki declaration and its later amendments or comparable ethical standards. The study protocol was approved by the Institutional Review Boards (IRBs) of St Marianna university hospital (No.4543). Written informed consent was obtained from patients. Although the analysis was retrospective and the confidentiality of the patients involved was protected. All patients' records/information was anonymized and de-identified prior to analysis.

References

- 1 Hasegawa J, Suzuki N. SMI for imaging of placental infarction. *Placenta*. 2016;47:96-8.
- 2 Hasegawa J, Kurasaki A, Hata T, Homma C, Miura A, Kondo H, et al. Diagnosis of placenta accreta spectrum using ultra-high-frequency probe and Superb Microvascular Imaging. *Ultrasound Obstet Gynecol*.

2019;54:705-7.

3 Furuya N, Hasegawa J, Homma C, Kawahara T, Iwahata Y, Iwahata H, et al. Novel ultrasound assessment of placental pathological function using superb microvascular imaging. *J Matern Fetal Neonatal Med.* 2020;1-4.

4 Hata T, Tanaka H, Noguchi J, Hata K. Three-dimensional ultrasound evaluation of the placenta. *Placenta.* 2011;32:105-15.

5 von Dadelszen P, Magee LA, Roberts JM. Subclassification of preeclampsia. *Hypertens Pregnancy.* 2003;22:143-8.

6 Arakaki T, Hasegawa J, Nakamura M, Takita H, Hamada S, Oba T, et al. First-trimester measurements of the three-dimensional ultrasound placental volume and uterine artery Doppler in early- and late-onset fetal growth restriction. *J Matern Fetal Neonatal Med.* 2020;33:564-9.

7 Amy Heerema-McKenney EP, Monique De Paepe. *Diagnostic Pathology: Placenta.* 2nd ed; 2018.

8 Ernst LM. Maternal vascular malperfusion of the placental bed. *Apmis.* 2018;126:551-60.

9 Burton GJ, Jauniaux E. Pathophysiology of placental-derived fetal growth restriction. *Am J Obstet Gynecol.* 2018;218:S745-s61.

10 Redline RW, Ravishankar S. Fetal vascular malperfusion, an update. *APMIS.* 2018;126:561-9.

11 Stanek J. Chorangiomas of Chorionic Villi: What Does It Really Mean? *Arch Pathol Lab Med.* 2016;140:588-93.

12 Altshuler G. Chorangiomas. An important placental sign of neonatal morbidity and mortality. *Arch Pathol Lab Med.* 1984;108:71-4.

Conflict of Interest: There are no conflicts of interest to declare.

Table 1. Characteristics of the participants

	Cases (n=34)
Maternal age (years)	33.5 (22–44)
Gravida	1.5 (1–4)
Para	0 (0–3)
Gestational weeks at ultrasound	33 (23–38)
Gestational weeks at delivery	34 (24–40)
Birth weight (g)	1754 (467–3102)
Apgar score at 1 min	8 (2–9)
Apgar score at 5 min	9 (4–10)
Umbilical artery pH	7.30 (7.10–7.47)

Table 2: Comparison of SMI findings with histological findings

Case	Background	Background	SMI findings	SMI findings			Histological
	FGR	PE	Infarction	Avascular villi	Congestion	Chorangiomas	Infarction
1	+	-	+	+	-	-	+
2	+	-	+	+	-	-	+
3	+	-	+	+	+	+	+
4	+	-	+	-	+	-	+
5	+	-	+	-	-	+	+
6	+	-	+	-	+	+	+

Case	Background	Background	SMI findings	SMI findings				Histological
7	+	+	+	+	+	-	+	
8	+	+	+	-	+	+	+	
9	+	+	-	-	-	-	-	
10	+	+	-	-	-	+	+	
11	-	+	+	-	-	-	+	
12	-	+	+	-	-	-	+	
13	-	+	-	+	+	+	+	
14	-	+	-	+	-	+	-	
15	-	+	-	-	-	-	-	
16	-	+	-	-	-	-	+	
17	-	+	-	-	-	+	+	
18	-	+	-	-	-	-	+	
19	-	+	-	-	-	+	+	
20	-	-	+	+	+	-	+	
21	-	-	+	+	-	-	-	
22	-	-	+	+	-	-	+	
23	-	-	+	+	-	-	+	
24	-	-	+	+	-	-	+	
25	-	-	+	-	+	-	-	
26	-	-	+	-	-	+	+	
27	-	-	+	-	-	+	+	
28	-	-	-	-	+	-	-	
29	-	-	-	-	+	-	+	
30	-	-	-	-	-	-	-	
31	-	-	-	-	-	-	-	
32	-	-	-	-	-	-	-	
33	-	-	-	-	-	-	-	
34	-	-	-	-	-	-	+	

Agreed with

SMI, superb microvascular imaging; FGR, fetal growth restriction; PE, preeclampsia

Table 3: Area under the curve for accuracy of antenatal ultrasound detection of placental pathological findings according to the clinical condition

	FGR	Preeclampsia	Others	Overall
Infarction	0.945	0.540	0.800	0.675
Avascular villi	0.785	0.780	0.920	0.675
Congestion	0.655	0.540	0.540	0.620
Chorangiomas	0.380	0.450	0.420	0.540

FGR, fetal growth restriction.

Figure legends

Figure 1: Normal placenta depicted using superb microvascular imaging

Villous blood vessels (villous trees) are depicted from the fetal surface (bottom) to the terminal villi (top). Large arrow, stem villi; small arrow, terminal villi. Slow blood flow in the intervillous space from the spiral

artery is also visualized like as "scatter," which matches the heart rate of the mother as the background of villous tree (triangle).

Figure 2: Ultrasound findings using superb microvascular imaging of abnormal placental pathology

1. **Infarction:** Neither the background "scatter" and "villous tree" were detected, resulting in an echoic space (triangle).
2. **Avascular terminal villi:** Only the background "scatter" is observed without normal villous trees.
3. **Dilatation of stem villi (Congestion):** The stem villi were clearly dilated compared with the surrounding villous stem vessels.
4. **Hyper-vascular terminal villi (Chorangiosis):** Terminal villi are highly echoic compared with standard villi and appear to be "fluffy" (triangle).

Figure 3: Pathological findings

1. **Infarction:** Infarctions show collapse of the intervillous space and associated villous aggregation and coagulative necrosis, and over time all nuclear structures disappear. They are accompanied by neutrophil infiltration.
2. **Avascular terminal villi:** Villous stromal-vascular karyorrhexis with disappearance of all blood vessels and uniformly fibrotic and vitrified stroma.
3. **Dilatation of stem villi:** Dilatation of stem villi is defined as the enlargement of a stem villous vessel > 4 times that of neighboring vessels of similar caliber.
4. **Hyper-vascular terminal villi:** At least [?] 10 blood vessels are found in one terminal or intermediate villus; [?] 10 of these villi are found in a visual field at 10x; and [?] 10 of them are found in [?] 3 random cotyledon sections.

Figure 4: Accuracy of antenatal ultrasound detection of placental pathologic findings

1. Receiver Operating Characteristic (ROC) curve predicting infarction
2. ROC curve predicting avascular villi
3. ROC curve predicting congestion
4. ROC curve predicting chorangiosis

Figure 5: Superb microvascular imaging findings and pathological findings in case of diffuse small infarctions diagnosed as avascular villi: (a) Avascular villi was suspected because of detection of only scatter without villous tree. (b) Diffuse small infarctions are detected pathologically.

Appendix

Appendix S1 : Normal placenta depicted using superb microvascular imaging (SMI)

Appendix S2 : Infarction depicted using superb microvascular imaging (SMI)

Appendix S3 : Avascular villi depicted using superb microvascular imaging (SMI)

Appendix S4 : Congestion of stem villi depicted using superb microvascular imaging (SMI)

Appendix S5 : Chorangiosis depicted using superb microvascular imaging (SMI)

Appendix S6 : Superb microvascular imaging (SMI) findings in case of diffuse small infarctions diagnosed as avascular villi

Figure 1

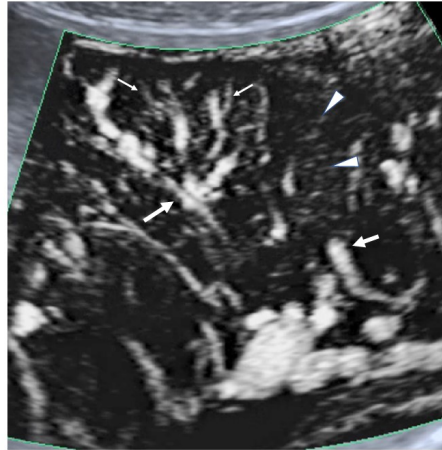


Figure 2

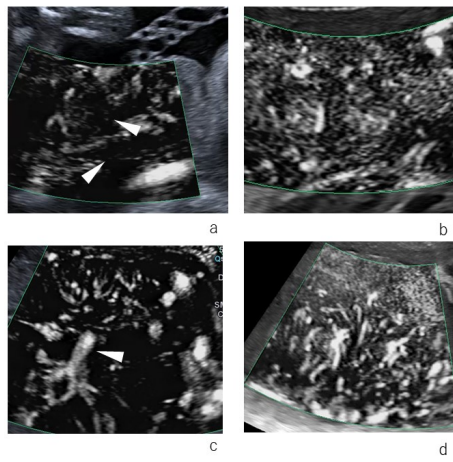


Figure 3

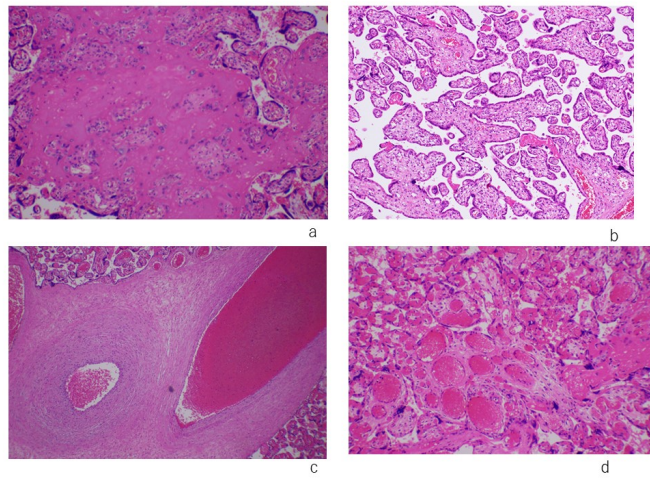


Figure 4a-b

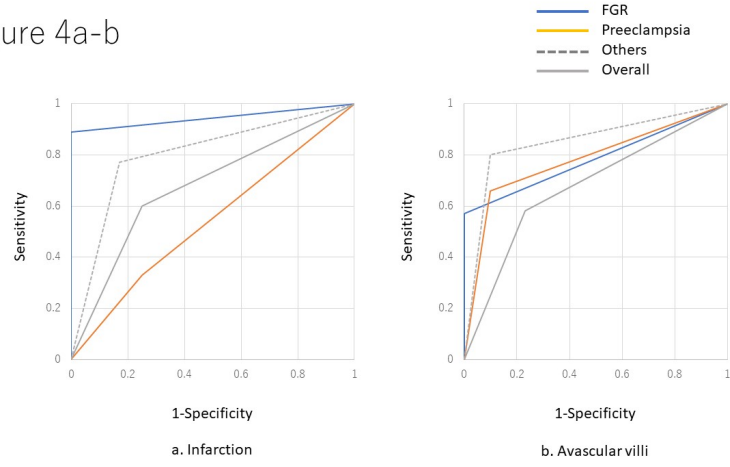


Figure 4c-d

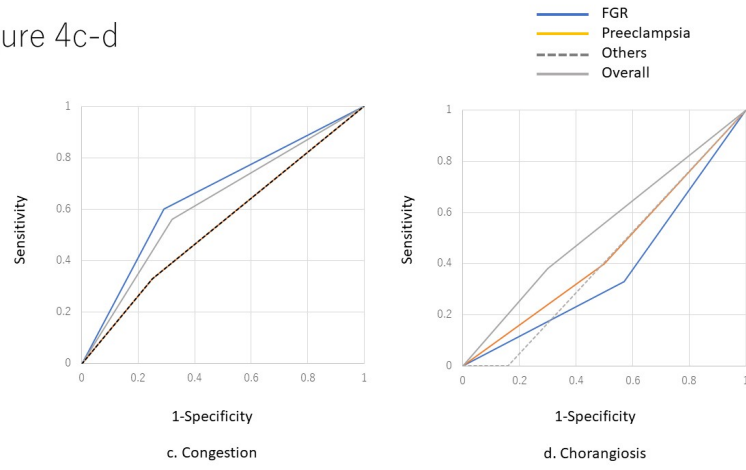
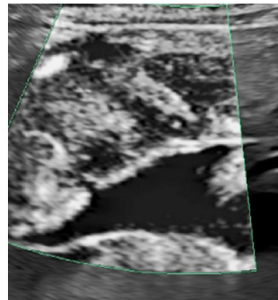
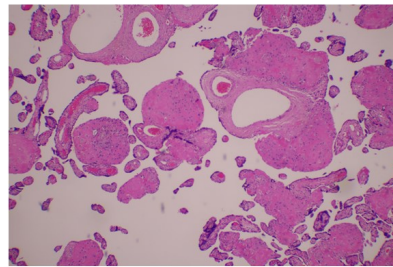


Figure 5



a



b